Fault-trapped waves depict continuity of the fault system responsible for the 6 April 2009 M_W 6.3 L'Aquila earthquake, central Italy

Giovanna Calderoni, Rita Di Giovambattista, Paola Vannoli, Stefania Pucillo, and Antonio Rovelli

Istituto Nazionale di Geofisica e Vulcanologia
Via di Vigna Murata 605
00143 Rome
Italy

Abstract

We investigate fault-trapped waves observed at a permanent broad-band station (FAGN) installed on the San Demetrio Fault, about 20 km southeast of L'Aquila. This fault has the same strike of the Paganica Fault which was responsible for the M_W 6.3, 6 April 2009 earthquake. The two faults display an en-echelon pattern with a few km offset. We have found that events causing efficient trapped waves are clustered at the northwestern and southeastern bottom ends of the ruptured Paganica fault plane. The efficiency of trapped waves at FAGN, which is located about 5 km far from the ruptured fault plane, indicates that the two faults are linked at depth. This suggests that fault segments in the study area can be part of a longer and continuous fault system which controls the seismic hazard of the region. Moreover, we have found that the two earthquake clusters generating the most efficient trapped waves occur in portions of the fault system with the highest fluid pressure.

Key words: 6 April 2009 L'Aquila earthquake, Paganica Fault, normal fault system, fault-zone trapped waves, fluid pressure, central Apennines

1) Introduction

On 6 April 2009 a M_W 6.3 earthquake struck the town of L'Aquila, central Apennines. The main shock was preceded by a long sequence of foreshocks since October 2008. After the main shock, two earthquakes with magnitude M_W 5.6 and 5.4 occurred within 4 days. The entire seismic sequence consisted of more than 20,000 aftershocks (Chiarabba et al., 2009; Di Luccio et al., 2010). The fault systems activated during the earthquake sequence are composed by sub-parallel NW-SE adjacent, west-dipping faults (e.g., Galadini et al., 2000; DISS Working Group, 2010).

The 6 April 2009 L'Aquila earthquake occurred in an area where a large number of well evident active faults had been mapped (Vezzani and Ghisetti, 1998, in red in Fig 1). However, the geometry of the individual faults and their structure at depth are poorly known. Although the Paganica Fault (PF) is largely accepted as the responsible for the M_W 6.3 main shock, the role of other neighboring faults in the rupture process is still debated (Falcucci et al. 2009; Boncio et al., 2010; Galli et al., 2010). This paper uses observations of fault-zone trapped waves (FZTWs) recorded on the San Demetrio Fault (SDF), southeast of the PF, to investigate the continuity of the fault system at depth.

FZTWs are seismic phases generated by constructive interference of critically reflected waves within low-velocity fault zones (Li and Leary, 1990; Li et al., 1990; Ben-Zion and Aki, 1990). These low velocity zones are originated by multiple competing and interacting factors such as dilatant cracks, fluids concentrated near faults, and increased porosity (Sibson, 1977; Wang, 1984; Li et al., 1990). Observations and modeling of FZTWs were often used to delineate the structure of faults at seismogenic depths (e.g., Li et al., 1994 and 1998; Hough et al., 1994; among many others). Lewis and Ben-Zion (2010) analyzed thousands of trapped wave seismograms recorded at on-fault stations along the Parkfield section of the San Andreas fault and concluded that i) events that generate FZTWs do not occur uniformly along the fault but are spatially clustered, and ii) events that generate FZTWs at one station do not necessarily generate them at other on-fault stations. Observations by Lewis and Ben-Zion (2010) imply that the damage zone is highly heterogeneous along strike and that a coherent connected wave guide does not exist everywhere along the fault. The study of FZTWs is therefore a powerful tool to infer information on uniform and continuous portions of the fault system.

In a recent paper, Calderoni et al. (2010) observed large amplitude FZTWs at a station (FAGN) installed on the SDF (Vezzani and Ghisetti, 1998), about 20 km southeast of L'Aquila (Fig. 1). Calderoni et al. (2010) found that the strongest effects were caused by events occurring in the southwest dipping fault plane near the station. They attributed them to heterogeneities at different scales controlled by the presence of the fault. In this paper, we reanalyze the same sequence of foreshocks and aftershocks to investigate if other portions of the fault system did generate efficient FZTWs at that station. We have found that events causing the most efficient trapped waves at FAGN are clustered at the northwestern and southeastern bottom ends of the fault plane responsible for the M_W 6.3, 6 April 2009 L'Aquila earthquake. These two clusters occur within seismogenic volumes characterized by the highest excess of fluid pressure as inferred through focal mechanism tomography (Terakawa et al., 2010). Thus our study provides further evidence of the role of fluids on the seismogenesis in the Apennines, as already proposed by other authors (Ghisetti and Vezzani, 2002; Chiodini et al., 2004; Miller et al., 2004; Ventura et al., 2007; Calderoni et al., 2009). Interestingly, FZTWs propagating from the northwestern edge of the 14-km-long seismogenic source are well recorded at FAGN which is southeast of causative shocks at distances of the order of 20 km, implying that these waves propagate coherently for more than 5 km out of the ruptured fault plane. This observation indicates that the trapping structure is continuous at depth beyond the PF and confirms that PF and SDF are part of a longer fault system.

2) Seismotectonic setting

Central Apennines suffered several of the strongest historical earthquakes in Italy. Earthquake catalogues (e.g. http://emidius.mi.ingv.it/CPTI08/) show the persistent occurrence of destructive earthquakes in this area: 9 September 1349 (M_W 6.5), 26 November 1461 (M_W 6.5), 2 February 1703 (M_W 6.7), 6 October 1762 (M_W 6.0). In the scientific community there is broad consensus that, according to the NE-SW extension (e.g., D'Agostino et al., 2011), the regional seismicity is mainly due to the activity of normal faults with NW-SE average strike (Vezzani and Ghisetti, 1998; Galadini and Galli, 2000; Valensise and Pantosti, 2001). The present day extensional regime follows the eastward migration of the Apennines compressional front, and the normal fault systems developed in areas previously affected by compression. The role played by the pre-existing compressional structures on the evolution and geometry of the active normal fault systems is still debated. However, there is a general agreement that active extension is accommodated by different sub-parallel NW-SE fault systems, composed by adjacent, southwest-dipping faults (e.g. Galadini et al., 2000; DISS Working Group, 2010). In contrast, there are open questions concerning the rate of activity of the numerous high-angle normal faults characterized by clear morphological scarps, well-preserved free-faces, and cataclasite zones that often border the Plio-Pleistocene intermountain basins. Basili et al. (2008) identify and characterize seismogenic sources at depth based on seismic, macroseismic and geological data, but the relationship between each seismogenic source and the overlying surface faults is object of debate.

The 6 April 2009, M_W 6.3 earthquake has further contributed to the debate about the mismatch between the deep source and its surface expression. The seismic sequence distribution depicts a SW-dipping fault plane from the hypocenter ($h \approx 10$ km) to 2-3 km of depth (Chiarabba et al., 2009), and the lack of seismicity shallower than 2-3 km does not allow to evaluate the correspondence between the fault imaged by seismicity and the surface faults. Nevertheless there is general consensus that the upward prolongation of the rupture plane with relatively low dip angle intersects the surface near the PF. This fault was a poorly known tectonic feature before April 2009 (Pace et al., 2006), with minor surface evidence (Bagnaia et al., 1989) and defined “uncertain or buried fault” in the digital version of the official geological maps (Servizio Geologico d’Italia, 2006). An extraordinary amount of seismological, geodetic, and geological data and analyses are available after the 2009 seismic sequence and give insights on the source complexity of the 6 April main shock. The analysis of these data led the DISS Working Group (2010) to characterize the source rupture plane that is consistent with the largest part of the collected data. This source has been identified as the Paganica Seismogenic Source (Fig. 1) that is a N-133°-striking, 14-km-long normal fault located at a depth between 3 and 9.5 km and the size of which is scaled to the seismic moment estimated by Herrmann et al. (2011) through modeling of broad-band seismogram waveforms. The inversion of GPS and SAR data yields the variable slip distribution on the fault plane, with only few centimeters of slip predicted on the more superficial portion of the fault (Atzori et al., 2009; Walters et al., 2009). This small amount of surface slip is consistent with faint field evidence of co-seismic ruptures. Some authors (EMERGEO Working Group, 2010; Cinti et al., 2011; Vittori et al., 2011) found open cracks and few centimeters of ground displacement along a 3-km-long segment of the PF whereas Falcucci et al. (2009) and Boncio et al. (2010) extend the fracture zone to 10 and 13 km, respectively. On the other hand, Galli et al. (2010) identify the Paganica-San Demetrio fault system, a 19-km-long structure, made up of seven main segments with a right-stepping *en-echelon* arrangement in three main sub-parallel splays, where the southern splay of the SDF does not show clear relationships with the other segments (Fig. 1). These authors propose that the 1461 earthquake is the twin of the 2009 event and identify the Paganica-San Demetrio fault system as the structure responsible for these earthquakes. Consistently, based on a macroseismic analysis, Tertulliani et al. (2010) suggest a similarity between the damaged areas of the 6 April 2009 earthquake with the 1461 and 1762 events (M_W 6.5 and 6.0, respectively; CPTI

Working Group, 2008). However, Di Bucci et al. (2011) remark the difficulty in locating these events owing to the small number of intensity data.

Paleoseismological analyses along the PF revealed the traces of the surface-faulting events, and show the occurrence of larger displacement events (Galli et al., 2010; Cinti et al., 2011). Although a portion of the difference in displacement is explained and documented by postseismic amplification of the throw due to afterslip along the fault, these larger displacements seem to be the evidence of larger magnitude paleo-earthquakes.

3) CLUSTERS GENERATING THE MOST EFFICIENT FAULT-TRAPPED WAVES

In this study, FZTWs detected by Calderoni et al. (2010) at the permanent broad-band seismological station of FAGN are reanalyzed in further detail to investigate if other portions of the fault system did generate efficient trapped waves thus to infer continuity of the fault zone at depth, with direct implications for hazard assessment of the region. The station is installed on the SDF that, according to the Vezzani and Ghisetti (1998) map, is aligned southeast of the PF; the two faults display an en-echelon pattern with a few km offset (Fig. 1). As discussed in Calderoni et al. (2010), a large amplification is observed in a broad frequency band (1-8 Hz) for tightly clustered shocks near FAGN, indicating a complex local effect controlled by the presence of the fault. They assessed the fault amplification through the spectral ratio between the two stations FAGN and AQU (Fig. 1), having demonstrated the suitability of this parameter to quantify the local ground motion anomaly of FAGN, after propagation distance compensation in terms of geometrical spreading. Using the analytical solutions by Ben-Zion and Aki (1990) and Ben-Zion (1998), Calderoni et al. (2010) investigated geometry and velocity contrast of the fault zone in a grid search approach, and concluded that the bulk of the fault trapping effect was caused by a 250-300 m wide channel of damaged rocks characterized by a 25-30% velocity reduction and large attenuation ($Q \approx 20$).

Although the seismic response of FAGN is complicated by the presence of very shallow heterogeneities, the effects of wave propagation in the fault zone can be recognized in seismogram waveforms and spectrograms. An example of efficient FZTWs recorded at FAGN is shown in Fig. 2 (upper panels) as compared to waveforms recorded at AQU. This figure (lower panels) demonstrates that efficient FZTWs can also propagate for longer distances, especially for causative earthquakes close to the mainshock hypocenter near L'Aquila. Further examples and details on waveforms observed at FAGN during the seismic sequence are discussed in the Supplementary Material.

In this paper we have modeled seismic wave propagation in a realistic southwest dipping normal fault (according to the fault plane solution by Herrmann et al., 2011). Our modeling applies the finite difference technique by Caserta (1998) propagating a point-source SH pulse localized in the middle of the fault zone. According to Calderoni et al. (2010), the fault zone is modeled as a 300-m wide uniform low-velocity, high-attenuation (Q=25) layer embedded in a hard rock half-space with a 30% velocity reduction (Fig. 3). Elastic and anelastic parameters of the model are listed in Table 1. We have varied the length of the propagation path in the fault to check to what extent the fault excitation can vary for causative earthquakes occurring in the fault at different distances from the receiver. In our 2D model the source depth is used as a proxy for the length of the lateral propagation path in the 3D reality. Panels in the right hand side of Fig. 3 compare the variation in fault excitation (smooth curves) resulting for sources at different distances from the station: source depths of 8 and 18 km in the model correspond to propagation paths of the order of 10 and 20 km, respectively. These figures indicate that fault-trapped waves excite the 1-3 Hz frequency band and the fault resonant frequency has a small dependence on the path length, at least in the distance variability range of the observed FZTWs. In the Supplementary Material, we discuss the sensitivity of the fault zone spectrum to variations of the propagation path length in the model.

Consistently with the spectral ratio method used for observations, the level of fault excitation in the model is estimated as a spectral ratio between on-fault and off-fault receivers at the surface, at symmetric distance from the source (FAGN and S_{REF} of Fig. 3). Full curves of the two panels in the right-hand side of Fig. 3 represent the fault resonance excitation as assessed through synthetic seismograms of FAGN and Sref, in two models with source depth of 8 and 18 km that simulate FZTWs traveling along source-to-receiver paths of the order of those shown in Fig. 2. Based on the spectral shape of the numerical simulations, we infer that the frequency band around 2 Hz is much more representative of the fault-zone excitation than the one (1-8 Hz) previously used by Calderoni et al. (2010). That frequency band was able to characterize the site response but likely includes other near-surface effects caused at high frequencies by shallow heterogeneities, especially for vertical incident shocks beneath FAGN. Therefore, we repeat the FAGN/AQU spectral ratio analysis as in Calderoni et al. (2010) but here spectral ratios are computed in the narrower frequency band 1 to 3 Hz. The efficiency of individual-event trapped waves is estimated as the mean value of the spectral ratio logarithm in this frequency band. Fig. 4a shows the pattern of FZTW efficiency as a function of the epicenters of causative earthquakes. It depicts significant variations for different shocks: the largest amplitudes occur for two clusters located at the bottom ends of the ruptured fault plane of the 6 April mainshock. The first is composed by 19 events and corresponds to the northwestern bottom end of the Paganica Seismogenic Source, beneath AQU (Fig. 1), where the main shock rupture nucleated. The second cluster (67 events) is substantially the same already identified by Calderoni et al. (2010) and corresponds to the southeastern bottom end of the Paganica Seismogenic Source.

The strong excitation of the fault zone resonance for the events of these clusters is documented with greater details in Fig. 5 where ground displacement spectra of stations AQU and FAGN are compared for events of the two clusters. All the spectra shown in Fig. 5 are scaled in amplitude to the low frequency (f < 1 Hz) plateau which is typical of the omega square source model below the corner frequency (Aki, 1967). In this way, the ground motion amplitude of the frequency band 1-3 Hz becomes independent of magnitude and distance of the causative earthquake. As a result, spectra of AQU obey the theoretical model, with a flat plateau at low frequency and a spectral decay above the corner frequency. In contrast, the displacement spectra of FAGN show an increase above the low-frequency plateau, in the narrow frequency band of the fault excitation: around 2 Hz the extra amplitude of FAGN is a measure of the FZTW efficiency, spectra of Fig. 5 having been normalized to 1 in terms of source radiation and distance.

In the two panels of the right-hand side of Fig. 3, we compare FAGN/AQU spectral ratios of the two clusters with the theoretical fault amplification for the two selected path lengths. The average spectra of the two clusters are both well fitted by spectra of synthetics within a 95% confidence interval. Although the uniform, constant width and velocity fault-zone model is a very rough approximation of the reality, it is able to reproduce the average data amplitude with a fairly good agreement. The spectral decay variation shown in Fig. 3 between the two clusters, consistently found both in the data behavior and synthetics, is a further evidence of the different propagation length in the low-Q fault zone of the FZTWs coming from the two clusters. Although some authors ascribe the fault zone trapping effect only to the shallowest part of the fault (e.g., Yang and Zhu, 2010; Yang et al., 2011), spectral variations of the FZTWs observed at FAGN are not consistent with a model where their origin is shallow since a shallow fault zone model would not produce any variation between the spectral shape of the two clusters. Moreover, earthquakes at distances of about 20 km from FAGN show approximately twice longer time delays than those for clustered aftershocks at ~10 km distances (Fig. 2), consistently with a continuous low-velocity waveguide between the clustered earthquakes and station FAGN.

4) Discussion and Conclusions

As observed by Savage (2010), variations in space might have a temporal origin. For this reason, we have plotted the trapped-wave efficiency in a graphic representation describing both time and space evolution. Fig. 4b shows the same amplitude parameter of Fig. 4a, but in this case the epicenters are projected on the AB cross-section that is parallel to the PF strike. Ordinate and abscissa axes represent individual-event position and origin time, respectively. Fig. 4b shows that the significant increase in the trapped-wave amplitude observed in the northwestern tip of the PF is also clustered in time and begins with the largest (M_W 4.1) foreshock of 30 March. The cluster in the southeastern tip was activated after the 6 April mainshock but there are no foreshocks in the same seismogenic volume to estimate an amplitude background value, then nothing can be concluded about possible temporal variations in this part of the fault. Furthermore, there is stringent evidence that only the events from these two spatially concentrated clusters promote large-amplitude FZTWs. According to Di Luccio et al. (2010), foreshocks were distributed along the hanging wall of the PF and migrated to the fault zone and in its footwall as the sequence evolved in time. A migration through the fault zone is consistent with a stronger excitation of FZTWs for earthquakes beginning with the 30 March foreshock.

Other authors (Di Luccio et al., 2010; Lucente et al., 2010; Telesca, 2010) observed the beginning of temporal changes in different seismic parameters starting from the 30 March foreshock. The temporal variations of FZTWs of the two clusters are faced in details in an ongoing study using repeating earthquakes of each cluster, here we focus on spatial features. One of the results is that the two clusters at the bottom ends of the Paganica Seismogenic Source correspond to deformed volumes characterized by the highest excess of fluid pressure as assessed by Terakawa et al. (2010) using focal mechanism tomography (Fig. 6). Although primary factors controlling efficiency of FZTWs are the position of the causative earthquake in the fault zone and focal mechanism (Fohrmann et al., 2004), fluids may have contributed to FZTW amplitude variations as well. Di

Luccio et al. (2010) and Lucente et al. (2010) enhanced the role of fluids during the seismic sequence resulting in a significant Vp/Vs increase after the 30 March foreshock. The role of fluids is also confirmed by geochemical surveys in two regional aquifers located in the epicentral area (Chiodini et al., 2011). Consistently, we have found that the two clusters of events generating the largest amplitudes of FZTWs (dots in Fig. 6) are fairly well correlated with the location of the high fluid pressure volume at depths between 7.5 and 10 km as shown by Terakawa et al. (2010). It is worthy of note that independent estimates (i.e. wave velocity of propagation paths and FZTW amplitudes) identify important changes of elastic parameters in the same seismogenic volume after the strongest foreshock.

The other result of this study is the continuity of the fault-zone at depth. The evidence of large-amplitude fault-trapped waves generated by earthquakes clustered at the bottom ends of the PF and recorded at FAGN, on the SDF, is a strong indication that the low-velocity wave-guide extends between the causative sources and the recording station. In particular, the efficient FZTW propagation from the northwestern cluster up to FAGN, about 20 km southeast, suggests that the wave guide extends for 6 km beyond the 14-km-long fault ruptured during the M_W 6.3, 6 April 2009 L'Aquila earthquake. This finding implies that PF and SDF, mapped as disjoint segments, are part of a longer and continuous fault system. This observation can have strong implications in terms of seismic hazard of the region since paleo-seismological evidences suggest that a sequential rupture of contiguous fault segments is likely producing earthquakes with magnitudes much larger than the 2009 event.

References

Aki, K., 1967. Scaling law of seismic spectrum. J. Geophys. Res. 72, 1217–1231, doi:10.1029/JZ072i004p01217.

Atzori, S., Hunstad, I., Chini, M., Salvi, S., Tolomei, C., Bignami, C., Stramondo, S., Trasatti, E., Antonioli, A., Boschi, E., 2009. Finite fault inversion of DInSAR coseismic displacement of the

2009 L'Aquila earthquake (central Italy). Geophys. Res. Lett. 36, L15305, doi:10.1029/2009GL039293.

Bagnaia, R., D'Epifanio, A., Sylos Labini, S., 1989. Aquila and Subequan basins: an example of Quaternary evolution in central Apennines, Italy. Quaternaria Nova 1, 1-23.

Basili, R., Valensise, G., Vannoli, P., Burrato, P., Fracassi, U., Mariano, S., Tiberti, M.M., Boschi, E., 2008. The Database of Individual Seismogenic Sources (DISS), version 3 - summarizing 20 years of research on Italy's earthquake geology. Tectonophysics 453, 20-43, doi:10.1016/j.tecto.2007.04.014.

Ben-Zion, Y., Aki, K., 1990. Seismic radiation from an SH line source in a laterally heterogeneous planar fault zone. Bull. Seismol. Soc. Am. 80, 971-994.

Ben-Zion, Y., 1998. Properties of seismic fault zone waves and their utility for imaging low-velocity structures. J. Geophys. Res. 103, 12, 567-12,585.

Boncio, P., Pizzi, A., Brozzetti, F., Pomposo, G., Lavecchia, G., Di Naccio, D., Ferrarini F., 2010. Coseismic ground deformation of the 6 April 2009 L'Aquila earthquake (central Italy, M_W 6.3). Geophys. Res. Lett. 37, L06308, doi:10.1029/2010GL042807.

Calderoni, G., Di Giovambattista, R., Burrato, P., Ventura, G., 2009. A seismic sequence from northern Apennines (Italy) provides new insight on the role of fluids in the active tectonics of accretionary wedges. Earth Planet. Sci. Lett. 281, 99-109, doi:10.1016/j.epsl.2009.02.015.

Calderoni, G., Rovelli, A., Di Giovambattista, R., 2010. Large amplitude variations recorded by an on-fault seismological station during the L'Aquila earthquakes. Evidence for a complex fault-induced site effect. Geophys. Res. Lett. 37, L24305, doi:10.1029/2010GL045697.

Caserta, A., 1998. A time domain finite-difference technique for oblique incidence of antiplane waves in heterogeneous dissipative media. Annali di Geofisica 41, 617-631.

Chiarabba, C., Amato, A., Anselmi, M., Baccheschi, P., Bianchi, I., Cattaneo, M., Cecere, G., Chiaraluce, L., Ciaccio, M.G., De Gori, P., De Luca, G., Di Bona, M., Di Stefano, R., Faenza, L., Govoni, A., Improta, L., Lucente, F.P., Marchetti, A., Margheriti, L., Mele, F., Michelini, A., Monachesi, G., Moretti, M., Pastori, M., Piana Agostinetti, N., Piccinini, D., Roselli, P., Seccia, D., Valoroso L., 2009. The 2009 L'Aquila (central Italy) M_W 6.3 earthquake: Main shock and aftershocks. Geophys. Res. Lett. 36, L18308, doi:10.1029/2009GL039627.

Chiodini, G., Cardellini, C., Amato, A., Boschi, E., Caliro, S., Frondini, F., Ventura, G., 2004. Carbon dioxide Earth degassing and seismogenesis in central and southern Italy. Geophys. Res. Lett. 31, L07615, doi:10.1029/2004GL019480.

Chiodini, G., Caliro, S., Cardellini, C., Frondini, F., Inguaggiato, S., Matteucci, F., 2011. Geochemical evidence for and characterization of CO2 rich gas sources in the epicentral area of the Abruzzo 2009 earthquakes. Earth Planet. Sci. Lett. 304, 389-398, doi: 10.1016/j.epsl.2011.02.016.

Cinti, F., Pantosti, D., De Martini, P.M., Pucci, S., Civico, R., Pierdominici, S., Cucci, L., Brunori C.A., Pinzi, S., Patera, A., 2011. Evidence for surface faulting events along the Paganica Fault prior to the April 6, 2009 L'Aquila earthquake (Central Italy). J. Geophys. Res. 116 (B07308), doi:10.1029/2010JB007988.

CPTI Working Group, 2008. Catalogo Parametrico dei Terremoti Italiani, versione parziale “CPTI08aq”. Istituto Nazionale di Geofisica e Vulcanologica, Milan, Italy. Available from http://emidius.mi.ingv.it/CPTI08/.

D’Agostino, N., Mantenuto, S., D'Anastasio, E., Giuliani, R., Mattone, M., Calcaterra, S., Gambino, P., Bonci, L., 2011. Evidence for localized active extension in the central Apennines (Italy) from global positioning system observations. Geology 39, 291-294, doi: 10.1130/G31796.1.

Di Bucci, D., Vannoli, P., Burrato, P., Fracassi, U., Valensise, G., 2011. Insights from the M_W 6.3, 2009 L’Aquila earthquake (Central Apennines) to unveil new seismogenic sources through their surface signature: the adjacent San Pio Fault. Terra Nova 23, 108-115.

Di Luccio, F., Ventura, G., Di Giovambattista, R., Piscini, A. Cinti, F.R., 2010. Normal faults and thrusts activated by deep fl uids: The 6 April 2009 M_W 6.3 L’Aquila earthquake, Central Italy. J. Geophys. Res. 115 (B06315), doi:10.1029/2009JB007190.

DISS Working Group, 2010. Database of Individual Seismogenic Sources (DISS), Version 3.1.1: A compilation of potential sources for earthquakes larger than M 5.5 in Italy and surrounding areas. http://diss.rm.ingv.it/diss/, © INGV 2010 - Istituto Nazionale di Geofisica e Vulcanologia, Rome, Italy

EMERGEO Working Group, 2010. Evidence for surface rupture associated with the M_W 6.3 L’Aquila earthquake sequence of April 2009 (central Italy). Terra Nova 22, 43-51, doi: 10.1111/j.1365-3121.2009.00915.x.

Falcucci, E., Gori, S., Peronace, E., Fubelli, G., Moro, M., Saroli, M., Giaccio, B., Messina, P., Naso, G., Scardia, G., Sposato, A., Voltaggio, M., Galli, P., Galadini, F., 2009. The Paganica fault and surface coseismic ruptures due to the April 6, 2009 earthquake (L’Aquila, Central Italy). Seismol. Res. Lett. 80, 6, doi:10.1785/gssrl.80.6.940.

Fohrmann, M., Igel, H., Jahnke, G., Ben-Zion, Y., 2004. Guided waves from sources outside faults: An indication for shallow fault zone structure?. Pure Appl. Geophys. 161, 2125-2137, doi:10.1007/s00024-004-2553-y.

Galadini, F., Galli, P., 2000. Active tectonics in the Central Apennines (Italy) - Input data for seismic hazard assessment. Natural Hazards 22, 225-270.

Galli, P., Giaccio, B., Messina, P., 2010. The 2009 central Italy earthquake seen through 0.5 Myr-long tectonic history of the L'Aquila faults system. Quaternary Science Reviews 29, 3768-3789.

Ghisetti, F., Vezzani L., 2002. Normal faulting, transcrustal permeability and seismogenesis in the Apennines (Italy). Tectonophysics 348, 155-168, doi:10.1016/S0040-1951(01)00254-2.

Herrmann, R.B., Malagnini, L., Munafò, I., 2011. Regional Moment Tensors of the 2009 L’Aquila Earthquake Sequence. Bull. Seismol. Soc. Am. 101, doi: 10.1785/0120100184.

Hough, S.E., Ben-Zion, Y., Leary, P.C., 1994. Fault-zone waves observed at the Southern Joshua Tree earthquake rupture zone. Bull. Seismol. Soc. Am. 8, 761-767.

Lewis, M.A., Ben-Zion, Y., 2010. Diversity of fault zone damage and trapping structures in the Parkfield section of the San Andreas Fault from comprehensive analysis of near fault seismograms. Geophys. J. Int. 183, doi:10.1111/j.1365-246X.2010.04816.x.

Li, Y.G., Leary, P.C., 1990. Fault zone trapped seismic waves. Bull. Seismol. Soc. Am. 80, 12451-12471.

Li, Y. G., Leary, P. C., Aki, K., Malin, P., 1990. Seismic trapped modes in the Oroville and San Andreas fault zones. Science 249, 763-766.

Li, Y.G., Vidale, J., Aki, K., Marone, C., Lee, W.K., 1994. Fine structure of the Landers fault zone: Segmentation and the rupture process. Science 265, 367-380.

Li, Y.G., Aki, K., Vidale, J.E., Alvarez, M.G., 1998. A delineation of the Nojima fault ruptured in the *M*7.2 Kobe, Japan, earthquake of 1995 using fault-zone trapped waves. J. Geophys. Res. 103, 7247-7263.

Lucente, F.P., De Gori, P., Margheriti, L., Piccinini, D., Di Bona, M., Chiarabba, C., Piana Agostinetti, N., 2010. Temporal variation of seismic velocity and anisotropy before the 2009 Mw 6.3 L'Aquila earthquake, Italy. Geology 38, 1015-1018, doi: 10.1130/G31463.1.

Miller, S.A., Collettini, C., Chiaraluce, L., Cocco, M., Barchi, M., Kaus, B.J.P, 2004. Aftershocks driven by a high-pressure CO2 source at depth, Nature 427, 724-727, doi:10.1038/nature02251.

Pace, B., Peruzza, L., Lavecchia, G., Boncio, P., 2006. Layered seismogenic source model and probabilistic seismic-hazard analyses in central Italy. Bull. Seism. Soc. Am. 96, 107–132, doi: 10.1785/0120040231.

Savage, M.K., 2010. The role of fluids in earthquake generation in the 2009 Mw 6.3 L'Aquila, Italy, earthquake and its foreshocks. Geology 38, 1055-1056; doi: 10.1130/focus112010.1.

Servizio Geologico d'Italia, 2006. Geological Map of Italy. Geological sheet n. 359 L'Aquila, scale 1:50,000, CARG Project, Agenzia per la Protezione dell'Ambiente e per i servizi Tecnici (APAT).

Sibson, R., 1977. Fault rocks and fault mechanisms. Journal of the Geological Society, 133, 191-213, doi:10.1144/gsjgs.133.3.0191.

Telesca, L., 2010. A non-extensive approach in investigating the seismicity of L'Aquila area (central Italy), struck by the 6 April 2009 earthquake (M_L 5.8). Terra Nova 22, 87-93.

Terakawa, T., Zoporowski, A., Galvan, B., Miller, S.A., 2010. High-pressure fluid at hypocentral depths in the L'Aquila region inferred from earthquake focal mechanisms. Geology 38, 995-998, doi: 10.1130/G31457.1.

Tertulliani, A., Rossi, A., Cucci, L., Vecchi, M., 2010. L'Aquila (Central Italy) Earthquakes: The Predecessors of the April 6, 2009 Event. Seism. Res. Lett. 80, 1008-1014, doi: 10.1785/ gssrl.80.6.1008.

Valensise, G., Pantosti, D., 2001. The investigation of potential earthquake sources in peninsular Italy: A review. Journal of Seismology, 5, 287-306.

Ventura, G., Cinti, F.R., Di Luccio, F., Pino, N.A., 2007. Mantle wedge dynamics versus crustal seismicity in the Apennines (Italy). Geochem. Geophys. Geosyst. 8, Q02013, doi:10.1029/2006GC001421.

Vezzani, L., Ghisetti, F., 1998. Carta geologica dell'Abruzzo, Scale 1:100,000, S.El.Ca., Florence, Italy.

Vittori, E., Di Manna, P., Blumetti, A.M., Comerci, V., Guerrieri, L., Esposito, E., Michetti, A.M., Porfido, S., Piccardi, L., Roberts, G.P., Berlusconi, A., Livio, F., Sileo, G., Wilkinson, M., McCaffrey, K.J.W., Phillips, R.J., Cowie, P.A., 2011. Surface Faulting of the 6 April 2009 Mw 6.3 L'Aquila Earthquake in Central Italy. Bull. Seism. Soc. Am., 101, 4, 1507-1530, doi:10.1785/0120100140.

Walters, R.J., Elliott, J.R., D'Agostino, N., England, P.C., Hunstad, I., Jackson, J.A., Parsons, B., Phillips, R.J. Roberts, G., 2009. The 2009 L'Aquila earthquake (central Italy): A source mechanism and implications for seismic hazard. Geophys. Res. Lett. 36, L17312, doi:10.1029/2009GL039337.

Wang, C.Y., 1984. On the constitution of the San Andreas fault zone in central California. J. Geophys. Res. 89, 5558-5866.

Yang, H., Zhu, L., 2010. Shallow low-velocity zone of the San Jacinto fault from local earthquake waveform modeling, Geophys. J. Int., 183, 421-432, doi:10.1111/j.1365-246X.2010.04744.x.

Yang, H., Zhu, L., Cochran, E.S., 2011. Seismic structures of the Calico fault zone inferred from local earthquake travel time modeling, Geophys. J. Int., 186, 760-770, doi: 10.1111/j.1365-246X.2011.05055.x.

5) Figure Captions

Figure 1: Map of the study area. White triangles are the two seismological stations used in this study; dots represent the epicenters of the analyzed foreshocks and aftershocks, those of the two clusters generating highest efficiency trapped waves are in red. The orange rectangle is the projection onto the surface of the ruptured fault plane responsible for the M_W 6.3, 6 April 2009 earthquake (the Paganica Seismogenic Source of DISS Working Group, 2010), red star indicates its epicenter. In red the active faults according to Vezzani and Ghisetti (1998), in yellow and in black the primary surface faults of the 6 April 2009 earthquake according to Falcucci et al. (2009) and Galli et al. (2010), respectively.

Figure 2: Examples of fault-parallel components and spectrograms of records characterized by a large amplitude phase in the frequency band 1-3 Hz that arrives to FAGN after direct S-waves. The time delay of this phase at FAGN is about 1 sec at source distances of the order of 10 km (event near FAGN, in the upper panels), and increases linearly for larger source distances (event near AQU, in the lower panels). There is no evidence of this phase at AQU.

Figure 3: (Left-hand side) Modeling of fault-trapped waves in a 60°-dipping normal fault. (Right-hand side) Fault-trapped wave amplification of synthetics (full curves) for sources at different distances (of the order of 10 and 20 km for events near FAGN and AQU, respectively) is compared to the average trend of seismograms (the mean spectral ratios of clusters at the north-western and south-eastern tips of the Paganica Fault is in the upper and lower panel, respectively).

Figure 4: (a) Pattern of individual-event amplification of trapped waves recorded at FAGN. The color scale of the epicenter symbols is proportional to the logarithm of the trapped wave amplification of that event, estimated through the geometric mean of the FAGN/AQU spectral ratio in the frequency band 1-3 Hz. The red rectangle is the surface projection of the Paganica Seismogenic Source. (b) Temporal variation of trapped-wave along the AB cross section. This representation enhances strong time variations triggered by the M_W 4.1, 30 March foreshock (indicated by the arrow) and confirms the spatial clustering of high-amplitude shocks at the edges of the ruptured fault plane. The dashed line marks the origin time of the 6 April main shock.

Figure 5: Ground displacement spectra (fault-parallel component) at stations FAGN and AQU for events of the two clusters that generated high efficiency trapped waves at FAGN. For each event, amplitudes are scaled to the flat displacement plateau as computed in the frequency band 0.5-1 Hz. A spectral bump centered around 2 Hz is evident at FAGN whereas AQU obeys the expected flat low-frequency displacement spectrum of the omega-squared theoretical model (Aki, 1967). In the bottom panels, the 95% confidence intervals of the spectra of the two stations are compared for each cluster.

Figure 6: (a) Perspective view of clusters generating efficient trapped waves at FAGN. (b) Map view of the excess fluid pressure distribution at depths of 7.5 km and 10 km (modified after Terakawa et al., 2010). Events of clusters exciting high-amplitude trapped waves (white diamonds) are superimposed on the fluid pressure maps.

***Highlights**

- We observe and model fault trapped waves during the 2009 L'Aquila sequence
- Two largest-amplitude clusters occur in fluid over-pressure zones at the fault tips
- Independent results yield changes of elastic parameters with the largest foreshock
- Seismic signals indicate that two ruptured fault segments are continuous at depth
- Close agreement to results on maximum magnitude coming from Paleoseismology

Figure 1
Click here to download high resolution image

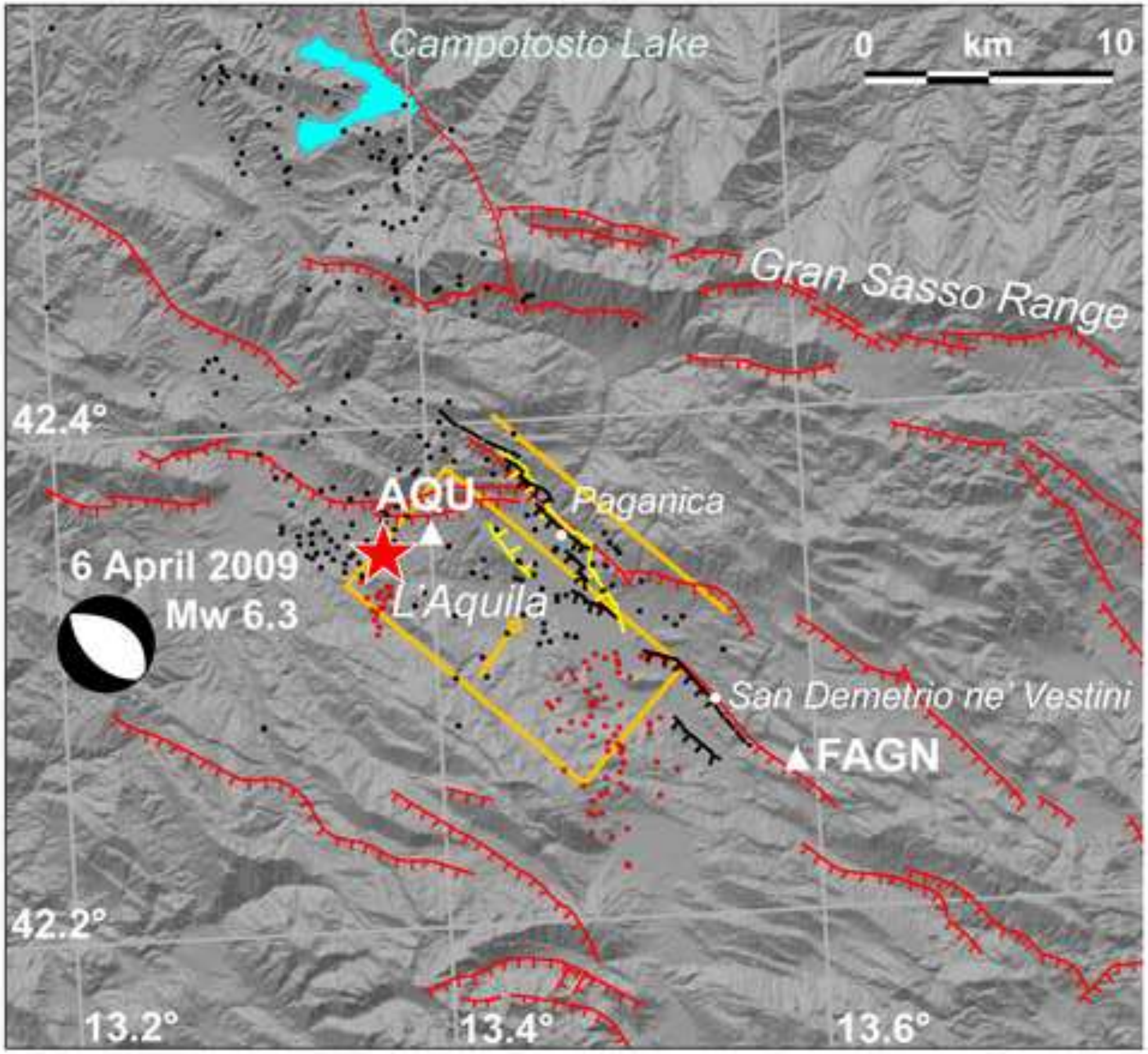

Figure 2

Click here to download Figure: Fig2.pdf

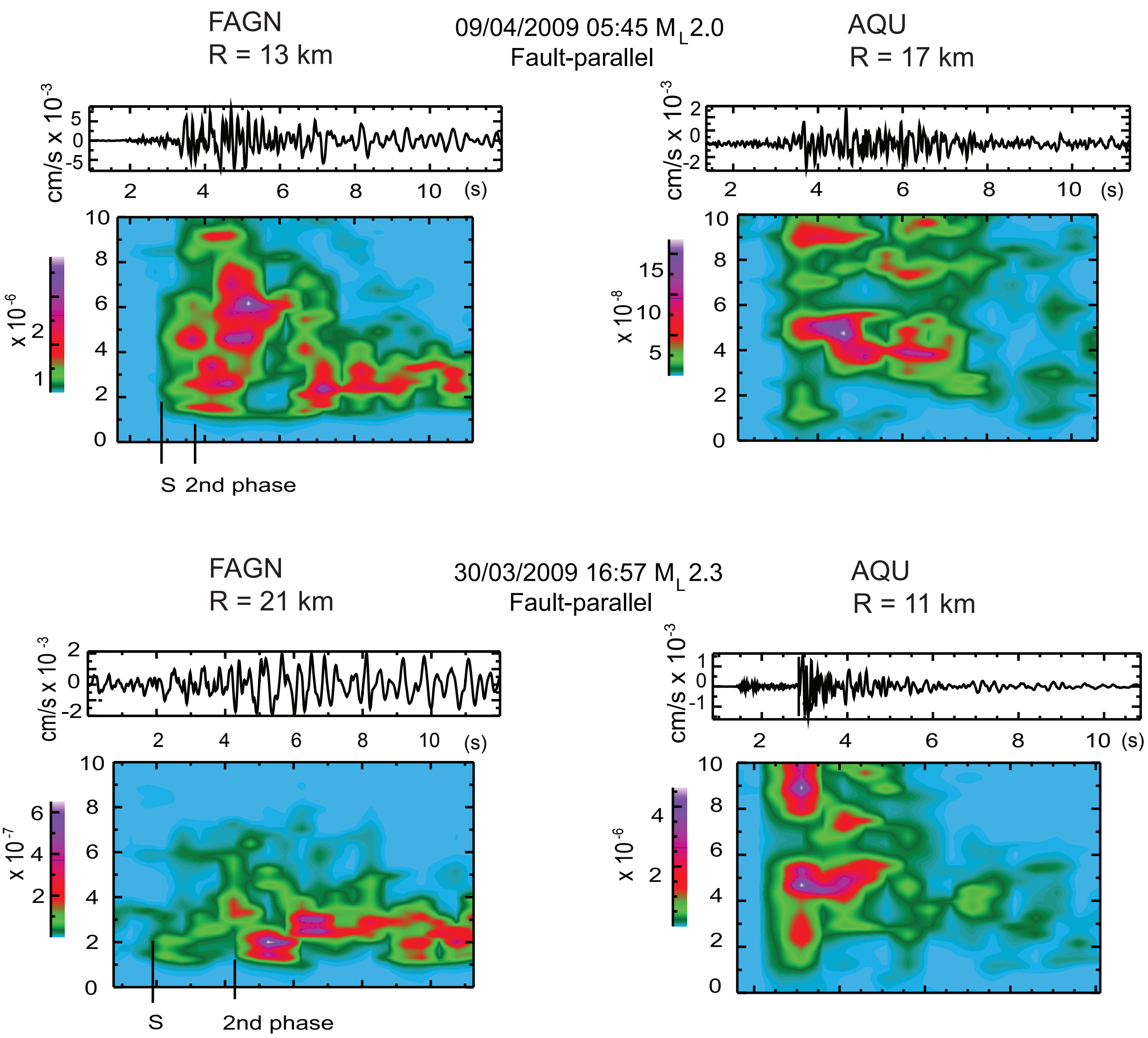

Figure 3
Click here to download Figure: Fig3.pdf

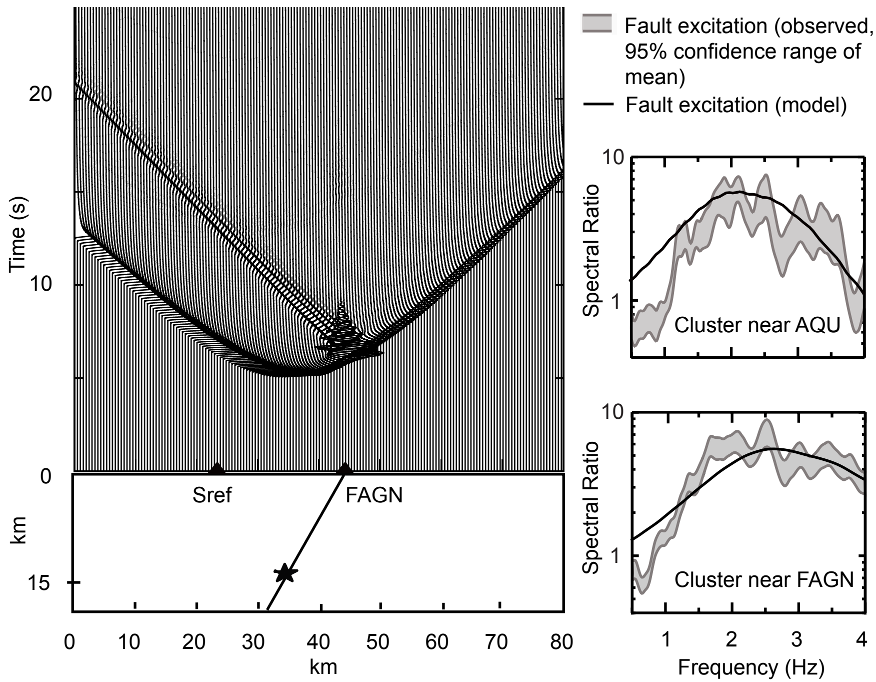

Figure 4
Click here to download high resolution image

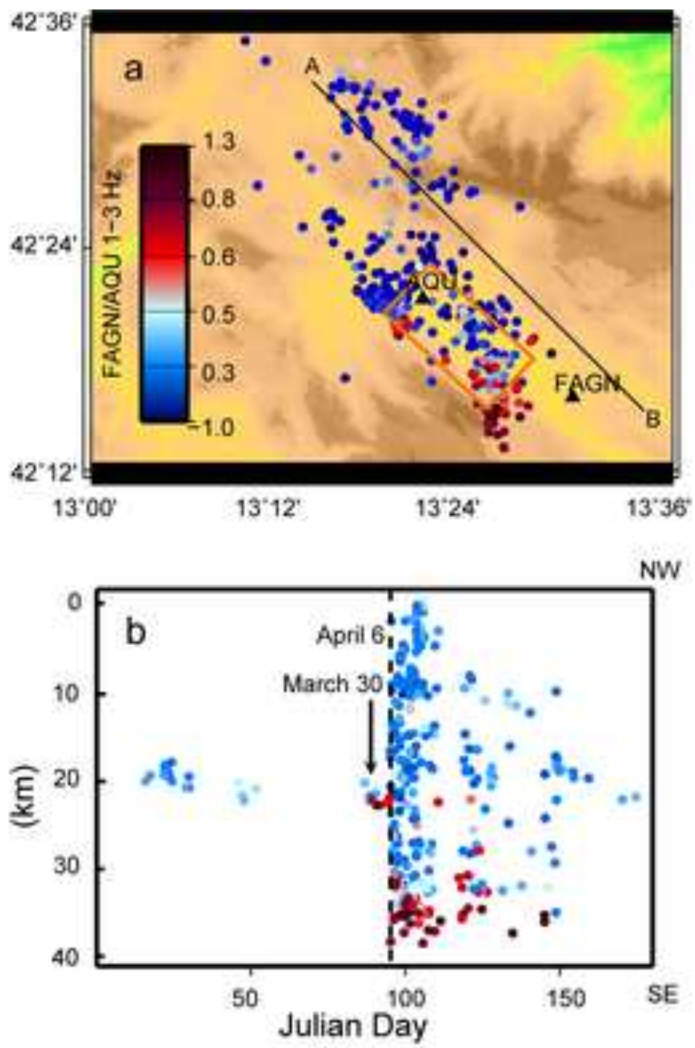

Figure 5
Click here to download Figure: Fig5.pdf

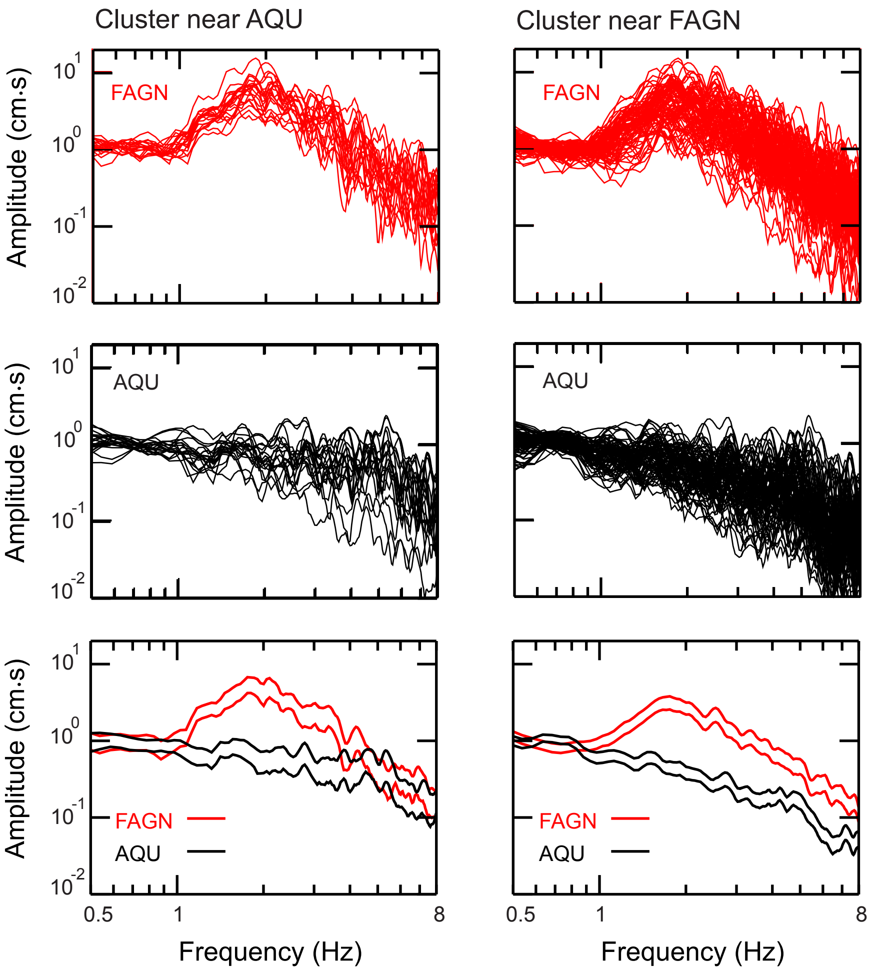

Figure 6

Click here to download Figure: Fig6.pdf

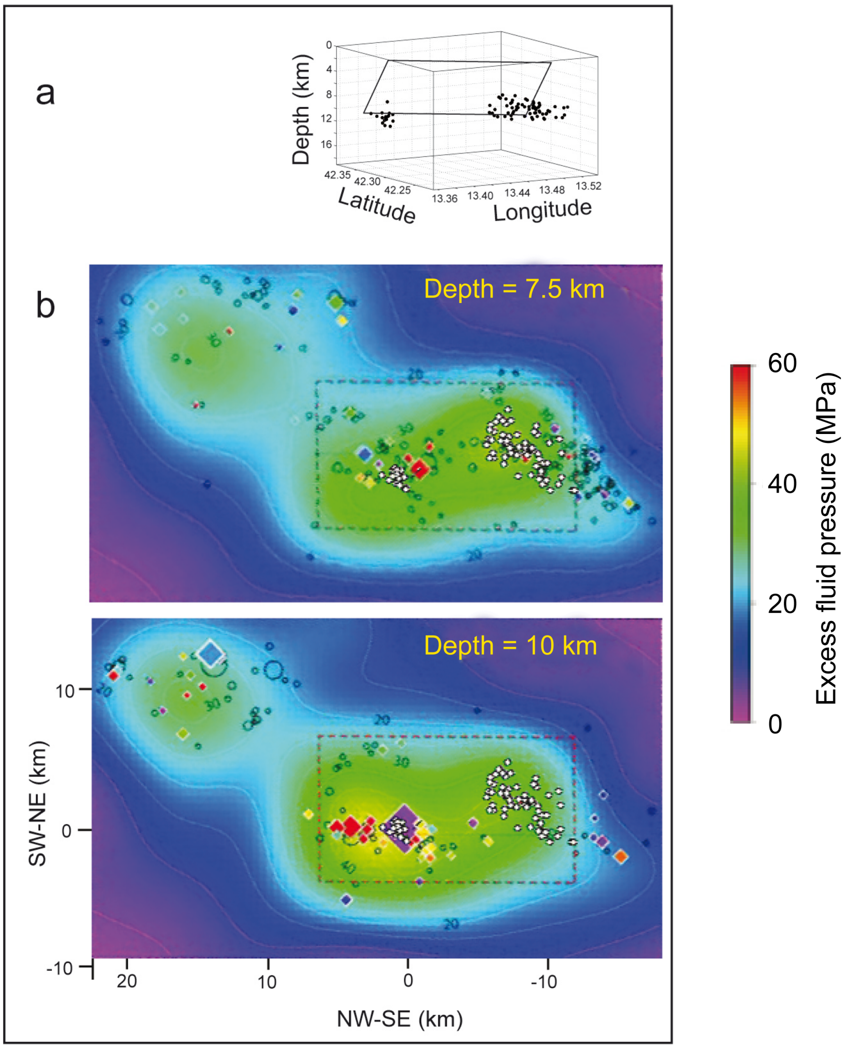

TABLE 1. Elastic and anelastic parameters of the numerical model

	Fault Zone	Half Space
Shear-wave velocity (km/s)	2.1	3.0
Density (g/cm^3)	2.4	2.6
Quality factor	25	100